Ionization of hydrogen molecular ions by antiproton impacts

Kazuhiro Sakimoto

Institute of Space and Astronautical Science, Japan Aerospace Exploration Agency, Yoshinodai, Sagamihara 229-8510, Japan

Ionization cross sections in collisions of antiprotons ($\bar{p}$) with H_2^+ molecules are calculated for incident energies in the range of 2–500 keV by using a semiclassical impact-parameter method. The electronic motion is solved in a numerically accurate manner by means of a discrete variable representation. A sudden approximation is applied to the description of the molecular rotation and vibration. The present $\bar{p}+H_2^+$ ionization cross sections are compared with the theoretical results of the ionization in $\bar{p}+He^+$ and the experimental results of the production of H^+ ions in $\bar{p}+H_2$.

PACS number(s): 34.50.Gb, 36.10.−k

I. INTRODUCTION

The ionization of atoms and molecules by antiproton ($\bar{p}$) impacts has become the subject of great theoretical and experimental interest. A lot of elaborate calculations have been carried out for ionization in $\bar{p}+H$ [1–14] and in $\bar{p}+He$ [15–23], and have offered the single-ionization cross sections in agreement with the experimental results [24–29] for incident energies $E \gtrsim 50$ keV. An interesting difference between the proton and antiproton impacts was experimentally recognized for the double-ionization cross sections of the He atom [24,25,28], and its origin could be explained by theoretical studies [15,27]. At low energies ($E<50$ keV), however, there still remain large discrepancies between the experimental and theoretical results both for the single- and double-ionization processes. Measurements were further made for ionization in $\bar{p}+H_2$ [28,30]. Again, a notable difference between the proton and antiproton impacts could be seen for the cross sections for production of the H^+ ion. In a theoretical aspect, on the other hand, little is investigated about the ionization of molecules by antiproton impacts.

The aim of the present paper is to perform an elaborate calculation of the ionization process for molecular targets. Although the H_2 molecule is the most desirable target for a detailed study, a reliable calculation of the two-electron system at $E \lesssim 100$ keV is still laborious even for the simplest case of the He atom target. In this paper, hence we focus on the ionization process in the one-electron system $\bar{p}+H_2^+$—i.e.,

$$\bar{p} + H_2^+ \rightarrow \bar{p} + H^+ + H^+ + e. \tag{1}$$

In the present case, the ionization of the H_2^+ molecule results in, at the same time, its dissociation by Coulomb repulsion. For the description of the electronic motion, we employ the direct numerical solution based on discrete variable representation (DVR) [31–34], which was already applied to the same system for the calculations of the electronic excitation probabilities in collinear collisions [35,36] and of the three-dimensional adiabatic potential energy surface useful for an understanding of the protonium ($\bar{p}p$) formation mechanism [37,38].

For the molecular target, we must consider the rotational and vibrational degrees of freedom, which often prevent us

from carrying out a complete theoretical calculation. Fortunately, the fact that the collision time is much shorter than the period of molecular rotation and vibration allows us to introduce a sudden approximation [39–41]. In this approximation, the internuclear distance and the molecular orientation remain fixed during the collision. The sudden approximation is commonly used for the calculation of electronic excitation in molecular collisions [42].

The present paper discusses the dependence of the ionization cross section on the internuclear distance and the molecular orientation, and reports the ionization cross section averaged over these quantities. Unfortunately, neither experimental measurements nor other theoretical calculations have been performed for ionization in $\bar{p}+H_2^+$. Here, comparison is made with the calculation for $\bar{p}+He^+$ [43] (He^+ being the united atom limit of H_2^+) and with the measurement for $\bar{p}+H_2$ [28].

II. THEORY

A. Impact-parameter method

A full quantum-mechanical calculation has now become possible as for ionization in the one-electron system of $\bar{p}+H$ [14]. In the present case of incident energies $E>1$ keV, however, a semiclassical impact-parameter method is believed to be highly accurate. We can assume that the $\bar{p}$ motion is given by a linear classical trajectory with a constant velocity V. The incident energy in the laboratory frame is given by $E=\frac{1}{2}\mu V^2$, with μ being the $\bar{p}$ mass (equal to the p mass). The effect of trajectory bending due to the Coulomb force between the antiproton and target ion is negligible when $E>1$ keV [44]. Here and in the following, we use atomic units unless otherwise stated.

We introduce the space-fixed frame (x,y,z), in which the z axis is chosen along the incident velocity and the $\bar{p}$ trajectory lies on the xz plane (Fig. 1). The positions of the three heavy particles are described in Jacobi coordinates $(\mathbf{R},\mathbf{r})$. The distance R is given by $R=\sqrt{b^2+V^2t^2}$, with b being the impact parameter and t the time. The polar and azimuthal angles of $\mathbf{r}$ are denoted by (θ,ϕ). We also introduce molecule-fixed frame (x',y',z'), in which the z' axis is chosen along the internuclear distance r (Fig. 1). Let $\mathbf{s}$ be the
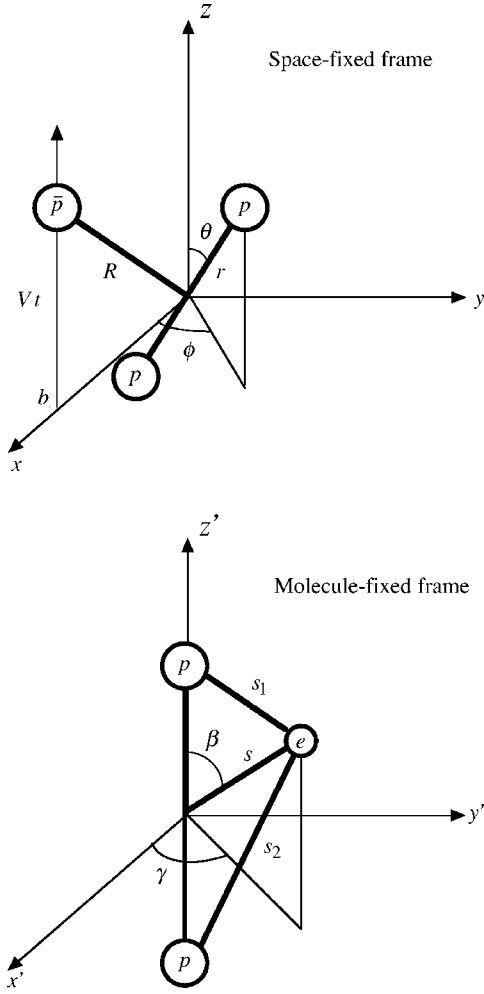
FIG. 1. Space-fixed and molecule-fixed frames.

position vector of the electron measured from the midpoint of r, and (β,γ) its polar and azimuthal angles in the molecule-fixed frame. The distances of the electron measured from the protons are denoted by s_1 and s_2, and the distance from the antiproton by s_3. In the molecule-fixed frame, the position vector $\mathbf{R}=(R_{x'},R_{y'},R_{z'})$ can be explicitly written as

$$R_{x'} = b\cos\theta\cos\phi - Vt\sin\theta,$$

$$R_{y'} = -b\sin\phi,$$

$$R_{z'} = b\sin\theta\cos\phi + Vt\cos\theta. \qquad (2)$$

The time-dependent Schrödinger equation is

$$i\frac{\partial}{\partial t}\widetilde{\Psi}(\mathbf{s},\mathbf{r},t) = H\widetilde{\Psi}(\mathbf{s},\mathbf{r},t). \qquad (3)$$

Here, the Hamiltonian H is divided into two parts:

$$H = H_0 + H_1, \qquad (4)$$

where

$$H_0 = -\frac{1}{2}\nabla_s^2 - \frac{1}{s_1} - \frac{1}{s_2} + \frac{1}{s_3} \qquad (5)$$

is the electronic part and

$$H_1 = -\frac{1}{\mu}\nabla_r^2 + \frac{1}{r} - \frac{1}{|\mathbf{R}+\mathbf{r}/2|} - \frac{1}{|\mathbf{R}-\mathbf{r}/2|} \qquad (6)$$

is related to the protons.

B. Sudden approximation

In the sudden approximation, we can simply set the wave function $\widetilde{\Psi}$ in the form [39]

$$\widetilde{\Psi}(\mathbf{s},\mathbf{r},t) = \Psi(\mathbf{s},t\!:\!\mathbf{r})\chi_{vj}(r)Y_{jm}(\theta,\phi), \qquad (7)$$

where χ_{vj} are the eigenfunctions of the molecular vibration, Y_{jm} the spherical harmonics, and (v,j,m) the initial vibrational and rotational quantum numbers. In the present study, only the ground state $(v,j)=(0,0)$ is considered. The wave function Ψ is the solution of the time-dependent equation

$$i\frac{\partial}{\partial t}\Psi(\mathbf{s},t\!:\!\mathbf{r}) = H_0\Psi(\mathbf{s},t\!:\!\mathbf{r}). \qquad (8)$$

The electronic channels of the target molecule can be represented by the Born-Oppenheimer (BO) states. Defining $\Psi_{\alpha\lambda}^{\mathrm{BO}}(\mathbf{s}\!:\!\mathbf{r})$ to be the BO wave functions with λ being the electronic magnetic quantum number and α denoting the other electronic states, we give the initial condition

$$\Psi(\mathbf{s},t=-\infty\!:\!\mathbf{r}) = \Psi_{10}^{\mathrm{BO}}(\mathbf{s}\!:\!\mathbf{r}), \qquad (9)$$

where $(\alpha,\lambda)=(1,0)$ indicates the ground BO state. The $\mathbf{r}$-dependent probability of the transition $(1,0)\to(\alpha',\lambda')$ is defined as

$$P(\alpha',\lambda'\!:\!\mathbf{r}) = \left| \int d\mathbf{s}[\Psi_{\alpha'\lambda'}^{\mathrm{BO}}(\mathbf{s}\!:\!\mathbf{r})]^*\Psi(\mathbf{s},t=\infty\!:\!\mathbf{r}) \right|^2, \qquad (10)$$

so that the $\mathbf{r}$-dependent ionization probability may be calculated from

$$P_{\mathrm{ion}}(r,\theta,\phi) = 1 - \sum_{\alpha'\lambda'}^{\mathrm{BS}} P(\alpha',\lambda'\!:\!\mathbf{r}), \qquad (11)$$

where the summation is taken over all electronic bound states (BS's). The ionization probability becomes

$$P_{\mathrm{ion}} = \int |\chi_{vj}(r)Y_{jm}(\theta,\phi)|^2 P_{\mathrm{ion}}(r,\theta,\phi)r^2\sin\theta dr d\theta d\phi. \qquad (12)$$

Since the probability (12) is evidently independent of the orientation of the impact parameter, the ionization cross section can be given by

$$\sigma = 2\pi \int P_{\mathrm{ion}}b\,db. \qquad (13)$$

For later convenience, we introduce the $\mathbf{r}$-dependent ionization cross sections

$$\sigma(r,\theta,\phi) = 2\pi \int P_{\text{ion}}(r,\theta,\phi) b \, db, \tag{14}$$

$$\sigma(\theta,\phi) = \int |\chi_{vj}(r)|^2 \sigma(r,\theta,\phi) r^2 dr, \tag{15}$$

$$\sigma(r) = \int |Y_{jm}(\theta,\phi)|^2 \sigma(r,\theta,\phi) \sin\theta \, d\theta \, d\phi. \tag{16}$$

As far as the electronic bound states are concerned, the Hamiltonian is practically invariant under reflection on the x-z plane (Fig. 1). Therefore, the ionization probability defined by Eq. (11) is invariant for the replacement $(\theta,\phi) \rightarrow (\theta, 2\pi - \phi)$. In addition, H_2^+ is a homonuclear molecule. From these facts, we can show the relation

$$\sigma(r,\theta,\phi) = \sigma(r, \pi - \theta, \pi + \phi) = \sigma(r, \pi - \theta, \pi - \phi), \tag{17}$$

and accordingly the range of the integration over ϕ in Eqs. (12) and (16) can be reduced to $0 \leq \phi \leq \pi/2$. The inversion symmetry is actually broken for the ionization process because the center of mass of H_2^+ is different from the midpoint of r. It should be noted that the invariance for $(\theta,\phi) \rightarrow (\theta, 2\pi - \phi)$ is valid only for the quantities integrated over the electronic continuum states, such as the total ionization probability (11).

If, for instance, r is always set to the mean internuclear distance $\bar{r}(=2.05 \text{ a.u.})$ like a rigid rotor or the r dependence of $\sigma(r,\theta,\phi)$ is negligible, the ionization cross section can be evaluated by Franck-Condon-type approximation

$$\sigma(\theta,\phi) \simeq \sigma_{\text{FC}}(\theta,\phi) = \sigma(\bar{r},\theta,\phi), \tag{18}$$

$$\sigma \simeq \sigma_{\text{FC}} = \sigma(\bar{r}). \tag{19}$$

This Franck-Condon approximation is often used for the calculation of electronic excitation in molecular collisions [42]. For the special case of $j=0$ considered in the present study, we can average over θ and ϕ according to

$$\sigma_{\text{FC}} = \frac{2}{\pi} \int_0^{\pi/2} d\phi \frac{1}{2} \int_0^{\pi} \sin\theta \, d\theta \, \sigma_{\text{FC}}(\theta,\phi). \tag{20}$$

C. Spheroidal coordinates

To describe the electronic motion in the $\bar{p}+H_2^+$ system, previous studies [36,37] introduced spheroidal coordinates (ξ,η,γ):

$$\xi = -r + s_1 + s_2, \quad 0 \leq \xi < \infty,$$

$$\eta = \frac{-s_1 + s_2}{r}, \quad -1 \leq \eta \leq +1,$$

$$\gamma = \gamma, \quad 0 \leq \gamma \leq 2\pi, \tag{21}$$

which are adapted to the two-center Coulomb nature of the H_2^+ molecule. Since the antiproton has a negative charge, two-center attraction among the electron and the protons is

the most important point to be considered in the numerical calculation.

Using the spheroidal coordinates, we can express the Hamiltonian H_0 as

$$H_0 = \frac{2}{G} \left[-\frac{\partial}{\partial\xi} \xi(2r+\xi) \frac{\partial}{\partial\xi} - \frac{\partial}{\partial\eta}(1-\eta^2)\frac{\partial}{\partial\eta} \right]$$
$$- \frac{2}{\xi(2r+\xi)(1-\eta^2)} \frac{\partial^2}{\partial\gamma^2} - \frac{1}{s_1} - \frac{1}{s_2} + \frac{1}{s_3}, \tag{22}$$

where

$$G(\xi,\eta) = \xi(2r+\xi) + r^2(1-\eta^2). \tag{23}$$

Splitting the wave function $\Psi(\mathbf{s},t:\mathbf{r})$ according to

$$\Psi(\mathbf{s},t:\mathbf{r}) = [\xi(2r+\xi)]^{-1/2} \psi(\xi,\eta,\gamma,t:\mathbf{r}), \tag{24}$$

we have from the time-dependent equation (8)

$$i\frac{\partial\psi}{\partial t} = (T+U)\psi, \tag{25}$$

where

$$T = \frac{2}{G} \left\{ -\xi(2r+\xi) \left[\frac{\partial^2}{\partial\xi^2} + \frac{1}{4\xi^2} \right] - \frac{\partial}{\partial\eta}(1-\eta^2)\frac{\partial}{\partial\eta} \right\}$$
$$- \frac{2}{\xi(2r+\xi)(1-\eta^2)} \frac{\partial^2}{\partial\gamma^2} \tag{26}$$

and

$$U(\xi,\eta,\gamma) = \frac{4r+\xi}{2G(2r+\xi)} - \frac{1}{s_1} - \frac{1}{s_2} + \frac{1}{s_3}. \tag{27}$$

We can show

$$-\frac{1}{s_1} - \frac{1}{s_2} = -\frac{4(r+\xi)}{G}. \tag{28}$$

The distance s_3 can be evaluated from $s_3 = |\mathbf{R}-\mathbf{s}|$ with use of expression (2). The explicit time dependence enters only through s_3 in the time-dependent equation (25).

III. NUMERICAL CALCULATIONS

A. Discrete variable representation

In the DVR method, the wave function is directly calculated on the grid points constructed from the zeros of orthogonal polynomials. The advantages of the DVR method are that the off-diagonal coupling matrix becomes sparse because it comes from only the kinetic energy terms, and in addition its matrix elements can be evaluated in purely algebraic form derived from the properties of orthogonal polynomials.

We use the generalized Laguerre polynomial $L_{n=N}^{(\alpha=1)}(\xi)$ for the grid ξ_i $(i=1,2,\ldots,N)$, the Legendre polynomial $P_{n=M}(\eta)$ for η_j $(j=1,2,\ldots,M)$, and the Chebyshev polynomial of the first kind $T_{n=2L+1}(u)$ with the argument $u=\cos[(\gamma+\pi)/2]$ for $\gamma_k=2\pi k/(2L+1)$ $(k=1,2,\ldots,2L+1)$. The choice of these orthogonal polynomials was explained in Refs. [36,37]. In

the present calculation, the consideration of $(2L+1)$ grid points for the γ coordinate means that the electronic angular momenta having $|\lambda| \leqslant L$ are actually included.

We expand the wave function ψ as

$$\psi(\xi, \eta, \gamma, t:\mathbf{r}) = \sum_{ijk} \psi_{ijk}(t:\mathbf{r}) f_i(\xi) g_j(\eta) h_k(\gamma), \quad (29)$$

where we have introduced the DVR basis functions

$$f_i(\xi) = \frac{[W(\xi)]^{1/2} L_N^{(1)}(\xi)}{\omega_i^{1/2} [dL_N^{(1)}(\xi_i)/d\xi](\xi - \xi_i)}, \quad (30)$$

$$g_j(\eta) = \frac{P_M(\eta)}{\omega_j^{1/2} [dP_M(\eta_j)/d\eta](\eta - \eta_j)}, \quad (31)$$

$$h_k(\gamma) = \frac{\omega_k^{1/2}}{2\pi} \sum_{\nu=-L}^{L} \cos[\nu(\gamma - \gamma_k)], \quad (32)$$

with $W(\xi) = \xi e^{-\xi}$ being the weight function of $L_N^{(1)}(\xi)$, ω_i the quadrature weight of $L_N^{(1)}(\xi)$ [45], ω_j that of $P_M(\eta)$ [45], and $\omega_k = 2\pi/(2L+1)$. The DVR basis functions satisfy the following relations:

$$f_i(\xi_{i'}) = \left[\frac{W(\xi_i)}{\omega_i} \right]^{1/2} \delta_{ii'}, \quad (33)$$

$$g_j(\eta_{j'}) = \omega_j^{-1/2} \delta_{jj'}, \quad (34)$$

$$h_k(\gamma_{k'}) = \omega_k^{-1/2} \delta_{kk'}, \quad (35)$$

and

$$\int_0^\infty f_i(\xi) f_{i'}(\xi) d\xi = \delta_{ii'}, \quad (36)$$

$$\int_{-1}^1 g_j(\eta) g_{j'}(\eta) d\eta = \delta_{jj'}, \quad (37)$$

$$\int_0^{2\pi} h_k(\gamma) h_{k'}(\gamma) d\gamma = \delta_{kk'}. \quad (38)$$

From Eqs. (33)–(35), the coefficients ψ_{ijk} in the expansion (29) turn out to be

$$\psi_{ijk}(t:\mathbf{r}) = \left[\frac{\omega_i \omega_j \omega_k}{W(\xi_i)} \right]^{1/2} \psi(\xi_i, \eta_j, \gamma_k, t:\mathbf{r}). \quad (39)$$

Expression (29) substituted into Eq. (25) leads to time-dependent linear equations for $\psi_{ijk}(t)$:

$$i\frac{\partial \psi_{ijk}}{\partial t} = \sum_{i'j'k'} T_{ijk,i'j'k'} \psi_{i'j'k'} + U(\xi_i, \eta_j, \gamma_k) \psi_{ijk}, \quad (40)$$

where the coupling matrix elements are

TABLE I. Variation of the ionization cross sections $\sigma(r, \theta, \phi)$ for $\bar{p} + H_2^+$, in units of a.u., with respect to L at $E=2$, 10, and 100 keV. The internuclear distance is $r=2.0$ a.u., and the molecular orientations are $(\theta, \phi) = (\pi/2, 0)$ and $(0, 0)$.

L	$E=2$ keV (30, 6)[a]	$E=10$ keV $(\theta,\phi)=(\pi/2,0)$ (30, 4)[a]	$E=100$ keV (20, 4)[a]
1	0.112	0.763	1.48
2	0.171	0.979	1.34
3	0.177	1.01	1.33
4	0.177	1.02	1.35

L	$(\theta,\phi)=(0,0)$ (30, 4)[a]	(20, 4)[a]	(20, 6)[a]
1	0.564	1.44	2.26
2	0.524	1.35	1.62
3	0.501	1.30	1.41
4	0.495	1.28	1.31
5		1.27	1.27
6			1.25

[a](N, M).

$$T_{ijk,i'j'k'} = -\frac{2\xi_i(2r + \xi_i)}{G(\xi_i, \eta_j)} \left\{ \delta_{jj'} \delta_{kk'} \int_0^\infty f_i(\xi) \left[\frac{\partial^2}{\partial \xi^2} + \frac{1}{4\xi^2} \right] \right.$$
$$\times f_{i'}(\xi) d\xi + \delta_{ii'} \delta_{kk'}$$
$$\left. \times \int_{-1}^1 g_j(\eta) \left[\frac{\partial}{\partial \eta} (1 - \eta^2) \frac{\partial}{\partial \eta} \right] g_{j'}(\eta) d\eta \right\}$$
$$- \delta_{ii'} \delta_{jj'} \frac{2}{\xi_i(2r + \xi_i)(1 - \eta_j^2)}$$
$$\times \int_0^{2\pi} h_k(\gamma) \frac{\partial^2}{\partial \gamma^2} h_{k'}(\gamma) d\gamma. \quad (41)$$

The integrals in this equation are evaluated in Refs. [32–34]. A set of $N \times M \times (2L+1)$ coupled equations (40) is solved by a fourth-order Runge-Kutta method.

B. Convergence behavior

The variations of the ionization cross section $\sigma(r, \theta, \phi)$ with respect to L, M, and N are shown in Tables I–III. The internuclear distance r is fixed to be the equilibrium value ($=2.0$ a.u.) of the H_2^+ molecule. In Table I, a choice of $L=3$ for the grid points γ_k is seen to yield cross sections with relative errors $|\Delta\sigma(r, \theta, \phi)/\sigma(r, \theta, \phi)|$ less than $\sim 2\%$ except for the case of $\theta=0$ at $E=100$ keV. Somewhat worse convergence for $\theta=0$ does not matter in the calculation of σ or σ_{FC} since $\sigma(r, \theta, \phi)$ is multiplied by the weight factor $\sin\theta$ in the integration over θ; cf. Eq. (16). For the convergence with respect to η_j (Table II), the relative errors of $<2\%$ are produced when $M \geqslant 6$ at the low energy $E=2$ keV and when $M \geqslant 4$ at the high energies $E \geqslant 10$ keV. Table III shows that, to obtain an accuracy of $\sim 2\%$ errors, we need $N=30$ or 40

TABLE II. Variation of the ionization cross sections $\sigma(r,\theta,\phi)$ for $\bar{p}+H_2^+$, in units of a.u., with respect to M at $E=2$, 10, and 100 keV. The internuclear distance is $r=2.0$ a.u., and the molecular orientation is $(\theta,\phi)=(\pi/2,0)$.

M	$E=2$ keV $(30, 3)^a$	$E=10$ keV $(30, 3)^a$	$E=100$ keV $(20, 2)^a$
2	0.217	1.00	1.04
4	0.185	1.01	1.34
6	0.177	1.00	1.37
8	0.175		1.36

$^a(N,L)$.

for ξ_i at the low energies $E \leq 10$ keV and the smaller value $N=20$ at the high energy $E=100$ keV.

In the present calculation of the ionization cross sections, we chose the number of grid points $(N,M,L)=(35,6,3)$ for low energies $(E \leq 50$ kev$)$ and $(N,M,L)=(20,6,4)$ for high energies $(E>50$ keV$)$. The total numbers of coupled equations to be solved are 1470 for $E \leq 50$ keV and 1080 for $E>50$ kev.

IV. RESULTS AND DISCUSSION

A. Dependence of the internuclear distance

We first examine the internuclear distance (r) dependence of the ionization cross section and ascertain the validity of the Franck-Condon (FC) approximation (18) or (19). Figure 2 shows the cross sections $\sigma(r,\theta,\phi)$ at $E=2$, 10, and 100 keV as a function of r in the range where the $(v,j)=(0,0)$ state has a non-negligible radial distribution $r^2|\chi_{vj}(r)|^2$ (cf. Fig. 3). The molecular orientations are chosen to be $(\theta,\phi)=(0,0)$, $(\pi/2,0)$, and $(\pi/2,\pi/2)$. For the orientation $(\pi/2,\pi/2)$, the cross section has very weak r dependence. For the other orientations, the cross section increases with r and takes much different values for the smallest and largest r shown in the figure. As seen in Table IV, however, the FC result $\sigma_{FC}(\theta,\phi)$ are very close to $\sigma(\theta,\phi)$ for all the orientations. This can be easily understood by the fact that the cross section has roughly a linear dependence on r. Namely, if we can assume that

TABLE III. Variation of the ionization cross sections $\sigma(r,\theta,\phi)$ for $\bar{p}+H_2^+$, in units of a.u., with respect to N at $E=2$, 10, and 100 keV. The internuclear distance is $r=2.0$ a.u., and the molecular orientation is $(\theta,\phi)=(\pi/2,0)$.

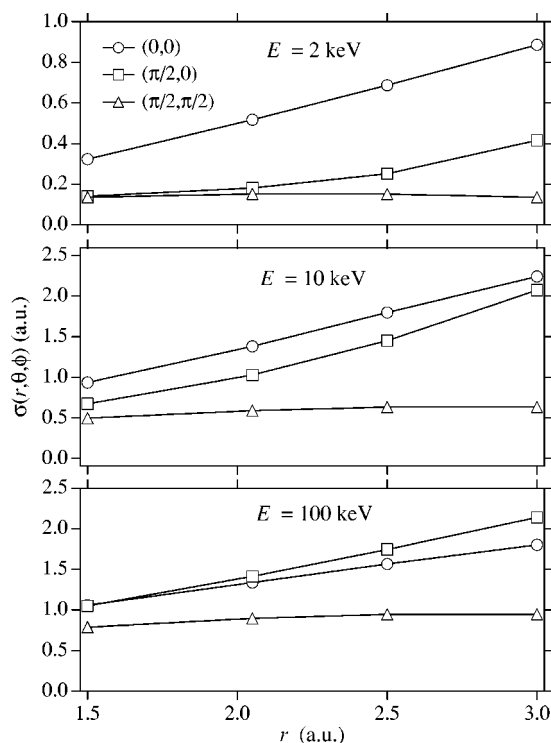| N	$E=2$ keV $(6, 3)^a$	$E=10$ keV $(4, 3)^a$	$E=100$ keV $(4, 2)^a$
10	0.151	1.19	1.46
20	0.172	1.03	1.34
30	0.177	1.01	1.34
40	0.172	0.984	1.32
50	0.173	0.978	

$^a(M,L)$.

FIG. 2. Ionization cross sections $\sigma(r,\theta,\phi)$ for $\bar{p}+H_2^+$, in units of a.u., as a function of the internuclear distance r at $E=2$, 10, and 100 keV. The molecular orientations are $(\theta,\phi)=(0,0)$, $(\pi/2,0)$, and $(\pi/2,\pi/2)$.

$$\sigma(r,\theta,\phi) = \sigma_{FC}(\theta,\phi) + \frac{d\sigma(\bar{r},\theta,\phi)}{dr}(r-\bar{r}) \qquad (42)$$

and further that $r^2|\chi_{vj}(r)|^2$ is an even function of $r-\bar{r}$ (cf. Fig. 3) as in the case of harmonic oscillator, then the Franck-Condon approximation becomes accurate. Anyway, it is certain that the Franck-Condon approximation is very good for
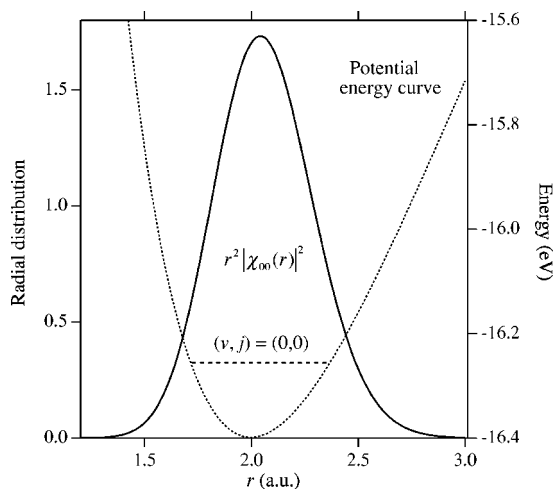

FIG. 3. Radial distribution $r^2|\chi_{v=0,j=0}(r)|^2$ of the H_2^+ molecular vibration, in units of a.u. The potential energy curve and the ground $(v,j)=(0,0)$ energy level of the H_2^+ molecule are also shown in units of eV.

TABLE IV. Comparison of the ionization cross sections $\sigma(\theta,\phi)$ and $\sigma_{FC}(\theta,\phi)=\sigma(\bar{r},\theta,\phi)$ for $\bar{p}+H_2^+$, in units of a.u., where $\bar{r}=2.05$ a.u. is the mean internuclear distance. The molecular orientations are $(\theta,\phi)=(0,0)$, $(\pi/2,0)$, and $(\pi/2,\pi/2)$, and the energies are $E=2$, 10, and 100 keV.

	$E=2$ keV	$E=10$ keV $(\theta,\phi)=(0,0)$	$E=100$ keV
$\sigma(\theta,\phi)$	0.523	1.40	1.34
$\sigma_{FC}(\theta,\phi)$	0.516	1.38	1.34
		$(\theta,\phi)=(\pi/2,0)$	
$\sigma(\theta,\phi)$	0.187	1.06	1.43
$\sigma_{FC}(\theta,\phi)$	0.181	1.03	1.41
		$(\theta,\phi)=(\pi/2,\pi/2)$	
$\sigma(\theta,\phi)$	0.150	0.588	0.892
$\sigma_{FC}(\theta,\phi)$	0.151	0.591	0.896

the calculation of the $\bar{p}+H_2^+$ ionization cross sections. We use the Franck-Condon approximation to carry out the subsequent discussions.

B. Dependence of the molecular orientation

Figure 4 shows the ionization cross sections $\sigma_{FC}(\theta,\phi)$ as a function of the polar angle θ for some given azimuthal angles ϕ up to $\pi/2$. The quantity $(\sin\theta)\sigma_{FC}(\theta,\phi)$, plotted in

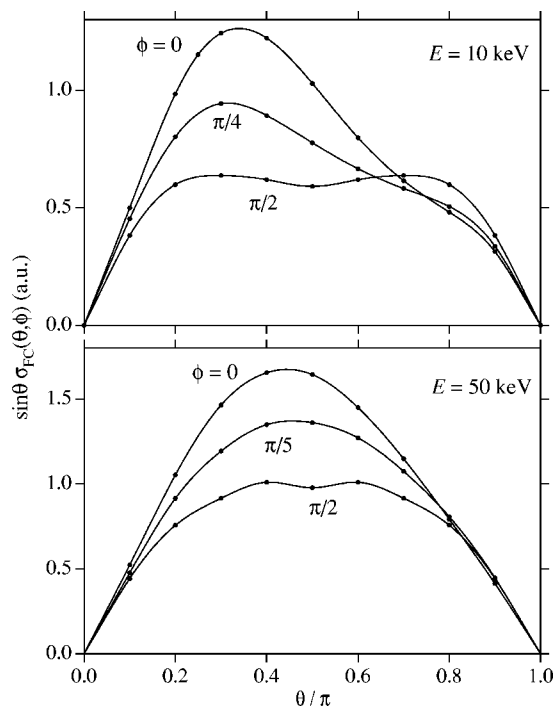FIG. 4. Ionization cross sections $\sigma_{FC}(\theta,\phi)$ times $\sin\theta$ for $\bar{p}+H_2^+$ in units of a.u., as a function of the polar angle θ. The azimuthal angles are $\phi=0$, $\pi/4$, and $\pi/2$ for $E=10$ keV and $\phi=0$, $\pi/5$, and $\pi/2$ for $E=50$ keV.
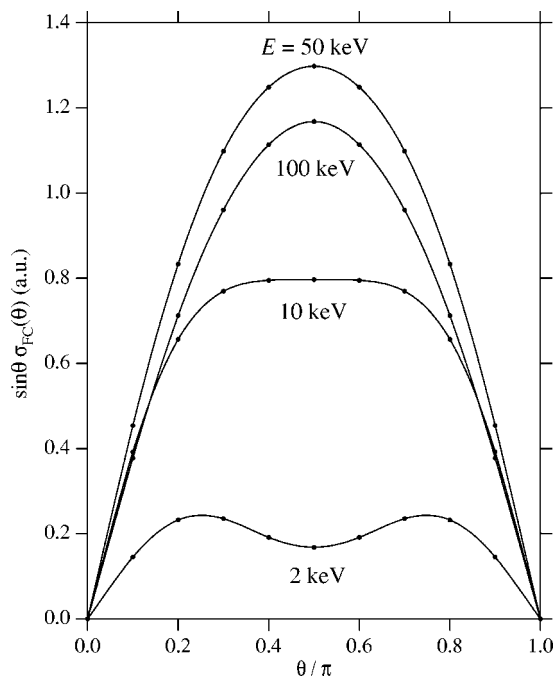

FIG. 5. Ionization cross sections $\sigma_{FC}(\theta)=\int_0^\pi \sigma_{FC}(\theta,\phi)d\phi/\pi$ times $\sin\theta$ for $\bar{p}+H_2^+$, in units of a.u., as a function of the polar angle θ at $E=2$, 10, 50, and 100 keV.

the figure, directly indicates which angle θ is important in the integration over θ. When $\phi=\pi/2$, the cross section becomes exactly a symmetric function of θ around $\theta=\pi/2$. The values of the cross section for $\phi>\pi/2$ can be evaluated by relation (17).

To see the preference of the polar angle θ for the ionization without respect to the ϕ dependence, we show the cross sections averaged over ϕ, $\sigma_{FC}(\theta)=\int_0^\pi \sigma_{FC}(\theta,\phi)d\phi/\pi$, in Fig. 5 for $E=2$, 10, 50, and 100 keV. The cross section $\sigma_{FC}(\theta)$ is always symmetric around $\theta=\pi/2$. At low energies, we find that polar angles $\theta<\pi/2$ (or $>\pi/2$) are relatively more important in the ionization. At high energies, however, the peak position of $\sin\theta\sigma_{FC}(\theta)$ becomes $\theta=\pi/2$. Therefore, we can conclude that a molecular orientation perpendicular to the $\bar{p}$ incident direction is preferable for the ionization at high energies and the nonperpendicular (or possibly nearly parallel) orientations are at low energies.

For the ϕ dependence, the ionization cross sections averaged over θ, $\sigma_{FC}(\phi)=\int_0^\pi \sigma_{FC}(\theta,\phi)\sin\theta d\theta/2$, are shown in Fig. 6 for $E=2$, 10, 50, 100, and 300 keV. On the whole, the ϕ dependence is not so strong. We can find that small azimuthal angles $\phi\sim0$ are more important for the ionization regardless of the energy. This simply implies that the ionization occurs more frequently as either of the protons becomes closer to the antiproton. At the intermediate energies ($E=10-100$ keV), the ionization cross section takes relatively large values and varies with ϕ in some measure. At the lowest ($E=2$ keV) and the highest ($E=300$ keV) energies, where the cross sections become small, however, we have a very weak ϕ dependence.

C. Ionization cross sections

The present results of the ionization cross sections σ_{FC} averaged over all the molecular orientations are displayed in
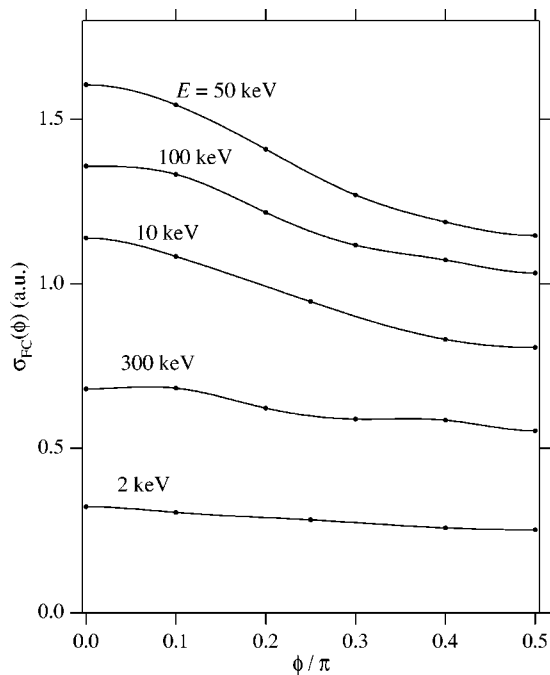
FIG. 6. Ionization cross sections $\sigma_{FC}(\phi)$ $=\int_0^\pi \sigma_{FC}(\theta,\phi)\sin\theta d\theta/2$ for $\bar{p}+H_2^+$, in units of a.u., as a function of the azimuthal angle ϕ at $E=2$, 10, 50, 100, and 300 keV.

Fig. 7. Since the H_2^+ molecule is regarded as being identical to the He^+ atom in the limit $r\to 0$, it is interesting to compare the present results with the ionization cross sections for $\bar{p}$ $+He^+$. The He^+ ionization cross sections calculated by Wehrman *et al.* [43] are also included in Fig. 7 and are much smaller than the present H_2^+ results. (Other recent calcula-
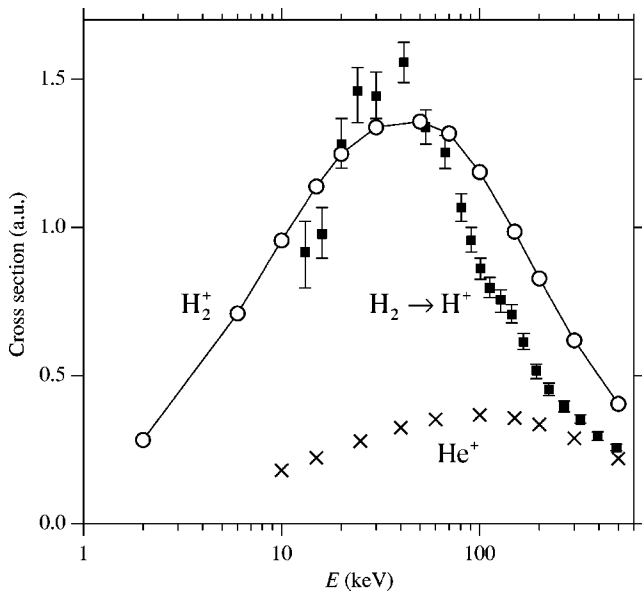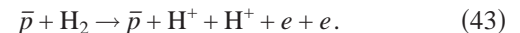

FIG. 7. Ionization cross sections σ_{FC} for $\bar{p}+H_2^+$, obtained in the present study, as a function of the incident energy E (○). Also shown are the theoretical ionization cross sections for $\bar{p}+He^+$, obtained by Wehrman *et al.* [43] (×), and the experimental results of the H^+ production in $\bar{p}+H_2$, obtained by Hvelplund *et al.* [28] (■). The cross sections are given in units of a.u.

tions for $\bar{p}+He^+$ [13,47–49] reasonably agree with the results of Wehrman *et al.*) As could be expected from Fig. 2, the ionization cross section would be the smallest for $r=0$. This can also be understood from the fact that the vertical ioniza-tion potential I of H_2^+ becomes small with increasing r: I $=54.4$ eV for $r=0$ (He^+), ~ 30 eV for $r\sim 2$ a.u., and $=13.6$ eV for $r=\infty$ (H). A similar feature for ionization can be observed in a comparison between $\bar{p}+H_2$ and $\bar{p}+He$ [28].

For the ionization in $\bar{p}+He$, Janev *et al.* [46] and later Wehrman *et al.* [43] suggested that the double ionization could be explained as a two-step sequential ionization pro-cess, and hence its cross section could be comparable to the single-ionization cross section for $\bar{p}+He^+$. In the case of $\bar{p}+H_2$, the double-ionization process produces the H^+ ion in the way

$$\bar{p}+H_2 \to \bar{p}+H^+ + H^+ + e + e. \qquad (43)$$

Since no data are available for the direct observation of Eq. (43), a comparison is made in Fig. 7 with the H^+ production cross sections for $\bar{p}+H_2$ measured by Hvelplund *et al.* [28]. We can find that the present single-ionization cross sections for $\bar{p}+H_2^+$ are very close to the H^+ production cross sections for $\bar{p}+H_2$. This fact may imply that the $\bar{p}+H_2$ double ioniza-tion can be explained in terms of the two-step sequential ionization as suggested by Janev *et al.* [46].

However, the H^+ ion can be produced in $\bar{p}+H_2$ also through the dissociative ionization channel

$$\bar{p}+H_2 \to \bar{p}+H + H^+ + e. \qquad (44)$$
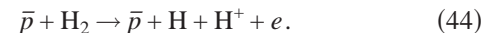
For electron or proton impacts on the H_2 molecule, the dis-sociative ionization occurs much more frequently than the double ionization [50,51]. It is not well understood whether this is also the case for the antiproton impacts [28,30]. To get some hint of the mechanism of the H^+ production in $\bar{p}+H_2$, we plot in Fig. 8 the present $\bar{p}+H_2^+$ results of the ionization probabilities $P_{ion}(\bar{r},\theta,\phi)$ and the excitation probabilities $P_{exc}(\bar{r},\theta,\phi)$ given by

$$P_{exc}(\bar{r},\theta,\phi) = 1 - P(\alpha=1,\lambda=0:\bar{r},\theta,\phi) - P_{ion}(\bar{r},\theta,\phi).$$
$$(45)$$

For the H_2^+ molecule, if the electronic excitation occurred vertically, the molecules in any electronic excited states would essentially dissociate ($\to H+H^+$) through the repulsive part of the potential energy curve [52]. Therefore, the exci-tation probability P_{exc} may be the lower limit of the disso-ciation probability. (The dissociation can also take place through the momentum-transfer process within the electronic ground state.) Figure 8 shows that the excitation occurs much more frequently than the ionization. This means that if the assumption of the two-step sequential process were ac-curate, the H^+ ion would be produced rather through the dissociative ionization (ionization+excitation). The similar-ity between the ionization in $\bar{p}+H_2^+$ and the H^+ production in $\bar{p}+H_2$, found in Fig. 7, would be merely accidental. Fur-ther study is needed for an understanding of the H^+ produc-tion mechanism in $\bar{p}+H_2$. In the present calculation, it might have been possible to obtain the cross sections for excitation in $\bar{p}+H_2^+$. As seen in Fig. 8, however, the calculation, requir-
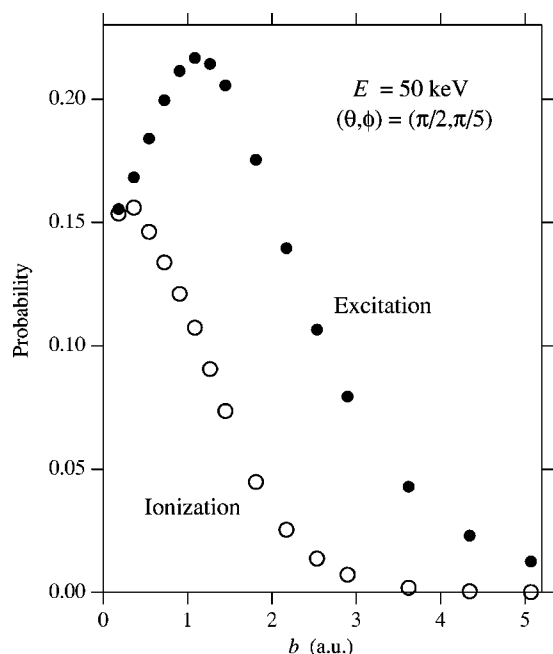
FIG. 8. Ionization probabilities $P_{ion}(\bar{r}, \theta, \phi)$ and excitation probabilities $P_{exc}(\bar{r}, \theta, \phi) = 1 - P(1, 0 : \bar{r}, \theta, \phi) - P_{ion}(\bar{r}, \theta, \phi)$ for $\bar{p} + H_2^+$ as a function of the impact parameter b. The molecular orientation is $(\theta, \phi) = (\pi/2, \pi/5)$, and the energy is $E = 50$ keV.

ing a wider range of impact parameters, would become extremely time consuming. Such a calculation remains in future work.

V. SUMMARY AND REMARKS

The most elementary ion-molecule collision system may be $\bar{p} + H_2^+$ because we can investigate the collision processes free of electron-correlation or electron-transfer effects. It is hence possible to carry out a considerably accurate calculation for this system. In the present study, the DVR method using spheroidal coordinates has been found useful. We have been able to produce the reliable ionization cross sections. Hopefully, measurements will be made soon for this system.

The internuclear distance and the molecular orientation dependence of the ionization cross section has been discussed in the framework of sudden approximation. The Frank-Condon approximation has been found to work very well for the rotational and vibrational ground state in the present system. To test the validity of the Frank-Condon ap-

proximation for rotational or vibrational excited states, we must investigate the r dependence of $\sigma(r, \theta, \phi)$ for both smaller and larger values of r. Nevertheless, $\sigma(r, \theta, \phi)$ is still expected to be roughly approximated by a linear function (42) even if the related range of r is somewhat wider than the present one. Probably, the Frank-Condon approximation will be good unless the rotational or vibrational state becomes very high.

The preference of the molecular orientation for ionization appears differently for low and high energies. The ionization cross section $\sigma(r)$ becomes large with the internuclear distance r. For the H_2^+ molecule, the mean internuclear distance $\bar{r}$ increases as the vibrational state becomes high. Hence, the Frank-Condon approximation says that the ionization cross section is larger for higher vibrational states. When the molecule is also in a rotational excited state, the mean internuclear distance becomes large owing to the centrifugal force. However, since the spherical harmonics are strongly dependent on θ for $j > 0$, the dependence of the ionization cross section on the rotational state cannot be easily conjectured.

As indicated in previous studies [35,36,53], when the energy is $\ll 1$ keV, the electronic excitation is negligible in the $\bar{p} + H_2^+$ collisions. In the region of such low energies, where $\bar{p}p$ formation and dissociation due to momentum transfer become the important reaction channels, the sudden approximation is of no use for the description of the molecular rotation and vibration, but alternatively the adiabatic (i.e., Born-Oppenheimer) approximation is fairly good for the electronic motion [35–37]. In the case of $\bar{p} + H_2$, however, the adiabatic approximation is invalid even at low energies [54]. A theoretical approach that can accurately treat the ionization process would be inevitable also for a physical understanding of $\bar{p}p$ formation in low-energy $\bar{p} + H_2$ collisions. The study of the $\bar{p} + H_2$ system is very interesting and challenging. Direct numerical solution of the time-dependent Scrödinger equation, like the present method, has now become possible for the two-electron system $\bar{p} + He$ [22]. In the near future, the development of computer ability will enable us to apply the present method to the calculation of the $\bar{p} + H_2$ collisions.

[1] D. R. Schultz *et al.*, Phys. Rev. Lett. **76**, 2882 (1996).
[2] J. C. Wells *et al.*, Phys. Rev. A **54**, 593 (1996).
[3] G. Schiwietz *et al.*, J. Phys. B **29**, 307 (1996).
[4] K. A. Hall *et al.*, J. Phys. B **29**, 6123 (1996).
[5] A. Igarashi *et al.*, Phys. Rev. A **61**, 062712 (2000).
[6] K. Sakimoto, J. Phys. B **33**, 3149 (2000).
[7] K. Sakimoto, J. Phys. B **33**, 5165 (2000).
[8] B. Pons, Phys. Rev. Lett. **84**, 4569 (2000).
[9] B. Pons, Phys. Rev. A **63**, 012704 (2001).
[10] X. Tong *et al.*, Phys. Rev. A **64**, 022711 (2001).
[11] N. Toshima, Phys. Rev. A **64**, 024701 (2001).
[12] J. Azuma *et al.*, Phys. Rev. A **64**, 062704 (2001).
[13] S. Sahoo *et al.*, J. Phys. B **37**, 3227 (2004).
[14] K. Sakimoto, Phys. Rev. A **70**, 064501 (2004).

[15] A. L. Ford and J. F. Reading, J. Phys. B **27**, 4215 (1994).

[16] J. F. Reading *et al.*, J. Phys. B **30**, L189 (1997).

[17] T. G. Lee *et al.*, Phys. Rev. A **61**, 062713 (2000).

[18] C. Díaz *et al.*, J. Phys. B **33**, L403 (2000).

[19] A. Igarashi *et al.*, Phys. Rev. A **62**, 052722 (2000).

[20] A. Igarashi *et al.*, Phys. Rev. A **64**, 042717 (2001).

[21] C. Díaz *et al.*, J. Phys. B **35**, 2555 (2002).

[22] D. R. Schultz and P. S. Krstić, Phys. Rev. A **67**, 022712 (2003).

[23] M. Keim *et al.*, Phys. Rev. A **67**, 062711 (2003).

[24] L. H. Andersen *et al.*, Phys. Rev. Lett. **57**, 2147 (1986).

[25] L. H. Andersen *et al.*, Phys. Rev. A **36**, 3612 (1987).

[26] L. H. Andersen *et al.*, Phys. Rev. A **41**, 6536 (1990).

[27] H. Knudsen and J. F. Reading, Phys. Rep. **212**, 107 (1992).

[28] P. Hvelplund *et al.*, J. Phys. B **27**, 925 (1994).

[29] H. Knudsen *et al.*, Phys. Rev. Lett. **74**, 4627 (1995).

[30] L. H. Andersen *et al.*, J. Phys. B **23**, L395 (1990).

[31] F. Calogero, J. Math. Phys. **22**, 919 (1981).

[32] J. C. Light *et al.*, J. Chem. Phys. **82**, 1400 (1985).

[33] D. Baye and P. H. Heenen, J. Phys. A **19**, 2041 (1986).

[34] D. T. Colbert and W. H. Miller, J. Chem. Phys. **96**, 1982 (1992).

[35] K. Sakimoto, Nucl. Instrum. Methods Phys. Res. B **214**, 131 (2004).

[36] K. Sakimoto, Phys. Rev. A **69**, 042710 (2004).

[37] K. Sakimoto, J. Phys. B **37**, 2255 (2004).

[38] K. Sakimoto, Chem. Phys. Lett. **393**, 245 (2004).

[39] D. M. Chase, Phys. Rev. **104**, 838 (1956).

[40] K. H. Kramer and R. B. Bernstein, J. Chem. Phys. **40**, 200 (1964).

[41] M. A. Wartell and R. J. Cross, Jr., J. Chem. Phys. **55**, 4983 (1971).

[42] V. Sidis, Adv. At., Mol., Opt. Phys. **26**, 161 (1989).

[43] L. A. Wehrman *et al.*, J. Phys. B **29**, 5831 (1996).

[44] P. S. Krstić *et al.*, J. Phys. B **29**, 1941 (1996).

[45] *Handbook of Mathematical Functions* edited by M. Abramowitz and I. E. Stegun, Natl. Bur. Stand. Appl. Math. Ser. 55 (U.S. GPO, Washington, DC, 1964).

[46] R. K. Janev *et al.*, J. Phys. B **28**, L615 (1995).

[47] D. R. Schultz *et al.*, Phys. Rev. A **56**, 3710 (1997).

[48] T. Kirchner *et al.*, Nucl. Instrum. Methods Phys. Res. B **154**, 46 (1999).

[49] X. Tong *et al.*, Phys. Rev. A **66**, 032708 (2002).

[50] I. Ben-Itzhak *et al.*, J. Phys. B **29**, L21 (1996).

[51] I. Ben-Itzhak *et al.*, J. Phys. B **34**, 1143 (2001).

[52] A. Carrington *et al.*, J. Phys. B **22**, 3551 (1989).

[53] J. S. Cohen, J. Phys. B **38**, 441 (2005).

[54] J. S. Cohen, Phys. Rev. A **56**, 3583 (1997).